ELSEVIER

Journal of Chromatography A, 789 (1997) 51–65

JOURNAL OF CHROMATOGRAPHY A

Enhancing the quality of information obtained by a comparison between experimental and deconvolved peak parameters in ion chromatography

P. Papoff[a,*], A. Ceccarini[a], F. Lanza[a], N. Fanelli[b]

[a]*Dipartimento di Chimica e Chimica Industriale, Via Risorgimento 35, 56126 Pisa, Italy*
[b]*Istituto di Chimica Analitica Strumentale del CNR, Via Risorgimento 35, 56126 Pisa, Italy*

Abstract

Chromatographic peaks are generally asymmetric owing to extra- and intra-column effects. This implies that the experimental retention time, $t_{R,p}$, and variance, σ_p^2, do not properly describe the shape of a peak under the experimental conditions used, nor do they allow one to predict how this shape will change when the composition of the eluent is varied. Consequently, some of the conclusions drawn from these experimental parameters may contain an extent of error that cannot be evaluated. This may occur for instance when some of the lower order statistical moments are used to estimate thermodynamic properties related to the solute–eluent–chromatographic column system. The aim of this paper is to test whether and to what extent information can be improved in ion chromatography when the moments estimated by some suitable fitting functions are compared to the experimental ones. The following fitting functions were tested: the exponentially modified Gaussian (EMG) (the peak deconvolution leads to the Gaussian curve which would be obtained in the absence of distortion), the bi-Gaussian (bi-G) (the deconvolution leads to the sum of two half-Gaussians), and the two-Gaussians (2-G) (the deconvolution leads to two Gaussians). The last one is proposed in this paper for the first time. Once we had evaluated how each component of a modern IC chromatograph (namely loop, column, post-column conditioning module and detector) affects the peak shape, the three fitting models were tested: (i) to compute β_1 and β_2 stability constants for the Cd^{+2}/Cl^- system from the measurement of the first-order moments at a variable Cl^- concentration and constant ionic strength (0.22). It was found that: $\beta_1=28.86$ (EMG), 28.53 and 28.59 (2-G), 28.99 (bi-G) and $\beta_2=57.96$ (EMG), 59.01 and 58.98 (2-G), 53.92 (bi-G). The β values calculated from the experimental retention times referred to the peak maximum were: $\beta_1=27.89$ and $\beta_2=64.95$; (ii) to evaluate, for the various solutes, the dependence on the first order moment (m_1) of some parameters of the i fitting functions, such as τ (the time constant of the exponential modifier in the EMG), σ_i (the square root of peak variance) and the asymmetry a/b (graphically measured as the ratio of the distances of the peak contour from the abscissa of peak maximum, at 0.1 peak height). A linear dependence on m_1 was found for: σ_i with a slope which depends on the fitting model used and not on the type of solute; τ and a/b with a slope which depends on the solute type. These findings are of interest: (i) to provide a sound tool for the accurate IC estimate of stability constants based on the Gaussian first order moment computed from the deconvolution of the experimentally distorted peak (ii) to evaluate how the shape of the solute peak changes with m_1 when the shift of the peak along the time (or volume) scale due to variations in the eluent composition can be thermodynamically predicted. In the last case the optimized peak separation conditions, which take the effect of peak shape variation into account, might be more efficiently found. © 1997 Elsevier Science B.V.

Keywords: Peak parameters; Gaussian curves; Peak shape analysis; Stability constants

*Corresponding author. Fax: +39 50 918260.

PII S0021-9673(97)00787-5

1. Introduction

Precise correlations are expected to be found in ion chromatography (IC) between the lower statistical moments of the elution peak of the cation under study and some independent variables, such as the nature and the concentration of competing ion or of a ligand. This occurs provided that the shape of the solute peak is a pure Gaussian and the elution mechanism is controlled by a linear exchange isotherm in the absence of multi-site adsorption mechanisms or kinetic effects [1].

The fact that experimental chromatographic peaks are usually asymmetrical is very often underestimated when the above mentioned correlations are being checked: this corresponds to assuming that the first and second order central moments pertain to a Gaussian profile over the whole range of experimental conditions adopted. This assumption is quite risky. It may be responsible for erroneous correlations between the expected and estimated stability constants as obtained from the shift in the experimental peak retention time ($t_{R,p}$) with a ligand concentration change [2,3].

We thus decided to test whether parameters, obtained from peak deconvolution, followed a theoretical behaviour, for a given solute–column–detector system, when the concentration of the competing ion or of the ligand was varied over a wide interval. In particular, we wanted to get accurate information on the relationship between the experimental and deconvolved peak parameters and the capacity factor k' which in turn depends on the eluent composition for a given solute and chromatographic column. Once this relationship has been found, the real possibility of obtaining accurate values of the stability constants from distorted peaks can be verified. A further aim was to improve the prediction of peak separation among different solutes by selecting a priori the eluent composition, whenever the variation in the experimental peak contour and the shift of retention time with eluent composition can be predicted for each solute.

Three alternative functions were used to fit skewed peaks: the exponentially modified Gaussian (EMG), the bi-Gaussian (bi-G) and the two Gaussian (2-G). The first two were widely used both to fit experimental chromatographic peaks and to separate overlapped peaks: they have never been tested, as far as we know, in searching for relationships between the parameters of a deconvolved peak and eluent composition over a large range of variation. The 2-G curve fitting function was selected because in some preliminary tests performed in our laboratory on GC and HPLC (both molecular or ionic) chromatograms, we found that any peak can be deconvolved into two Gaussians with a very good coincidence between computed and experimental curves.

This paper focuses on the effect of competing ion or ligand concentrations on deconvolved peak statistical moments. The data relevant to the Cd^{+2}/Cl^{-} system, which we had previously considered [3] for the determination of stability constants from the experimental retention time shift, were used along with those relevant to the alkaline ions to test the quality of information that deconvolved peak parameters can provide.

1.1. Different approaches to chromatographic peak shape analysis

In this section some significant papers on chromatographic peak shape analysis will be briefly reviewed to show the framework in which our research was carried out. More detailed information can be found in specific reviews.

The form (trailing or fronting edge) and the extent of peak asymmetry are generally ascribed to two main causes: (i) the effects that arise inside the chromatographic column (intra-column effects) [1]; (ii) the extra-column effects such as the dead volume, the injection volume, and the detector time constant [4–6]. The most common approach to peak shape analysis consists in considering only one of these causes at a time and in proposing sets of equations suited for estimating peak parameters or reproducing the original peak shape. In all cases the equations proposed to describe peak shape were non-linear and multiparametric. In principle this may imply that even an excellent fit to experimental chromatographic data can be obtained by different sets of equation parameters.

In the case of non-linear sorption isotherms [7], equations were derived on theoretical grounds in order to predict the chromatographic peak contour, according to the isotherm and column characteristics.

When the isotherm can be expressed by a parabolic equation, it was found that the efficiency of the column affects the front of the peak in a convex isotherm (the rear of the peak in a concave one) so that it tends to a vertical one as the plate number (N) gets higher. In all the cases considered in [7], the degree of coincidence between experimental and computed curves is fairly good, at least for the peak front. This implies that the parameters of the non-linear isotherm can be estimated by experimental measurements. When one-site or two-site Langmuir isotherms are considered [8], a fairly good coincidence between simulated and experimental curves is always observed, regardless of the model considered. In such cases the equation parameters assume the meaning of empirical coefficients and the possibility of enlightening the actual sorption mechanisms is lost.

As for the extra-column effects, an exponentially modified Gaussian (EMG) equation has been by far the most commonly used in computer deconvolution of skewed chromatographic peaks [4,6,9–11]. Some papers on EMG theory are devoted to computer simulation [11–13], while in others [4,6,9,14,15] the computed and experimental data are compared within the considered range of experimental conditions. Two interesting approaches to the calculation of peak parameters from experimental data are: Yau's algorithm [10] and Barber and Carr's graphical method [12]. In the last method the EMG parameters are evaluated by measuring the experimental retention time $t_{R,p}$, the width of the peak and the distances of the peak contour from $t_{R,p}$ at the selected fraction of the peak height.

The following equation was used in this paper for EMG peak deconvolution [10,11]:

$$h(t) = \frac{A}{\tau\sigma\sqrt{2\pi}} \int_0^{\infty} \exp\left(-\frac{(t - t_R - t')^2}{2\sigma^2} \right) \times \exp\left(-\frac{t'}{\tau} \right) dt' \quad (1)$$

where t' is a dummy integration variable, σ and t_R are respectively the standard deviation and the retention time of the Gaussian component of the peak, and τ is the time constant of the exponential modifier. The relevant four fundamental peak parameters which can be obtained by deconvolution are: the area A, the constant τ as well as the retention time t_R and the standard deviation σ.

When the bi-G and 2-G fitting functions are used, the fitting is performed by using two Gaussian curves.

In the bi-G the parameters of the first Gaussian are used within the $-\infty$, $-z_m$ interval (where z is the distance coordinate in time or volume units and z_m is the coordinate of peak maximum) and the parameters of the second Gaussian in the z_m, $+\infty$ interval according to the following equation [16]:

$$b(z) = \begin{cases} \dfrac{m_1}{\sigma_1\sqrt{2\pi}} \exp\left[-\dfrac{(z - z_m)^2}{2\sigma_1^2} \right] & -\infty < z \le z_m \\ \dfrac{m_2}{\sigma_2\sqrt{2\pi}} \exp\left[-\dfrac{(z - z_m)^2}{2\sigma_2^2} \right] & z_m \le z \le +\infty \end{cases} \quad (2)$$

In this case the zeroth moment (total peak area) m_0 is given by $m_0 = 1/2(m_1 + m_2)$, the first order moment (peak mean coordinate) is equal to $z_m + (2/\pi)^{1/2}(\sigma_2 - \sigma_1)$ and the second order moment (σ^2) is given by

$$\sigma^2 = \left(\frac{\sigma_1 + \sigma_2}{2} \right)^2 + \frac{3\pi - 8}{4\pi}(\sigma_2 - \sigma_1)^2.$$

Owing to the impossibility of testing this function with the different experimental types of skewed peaks, Buys and De Clerk [16], used the normalized Poisson distribution:

$$F(z) = \frac{1}{b^{n+1}(n!)} z^n \exp(-z/b) \quad (3)$$

by changing the b and n parameters. As for the ratio of zeroth order moments

$$\frac{m_0(bi\text{-}G)}{m_0(\text{Poisson})}$$

they observed that a 4% maximum relative error was obtained for $n = 1$, corresponding to a highly distorted peak[1]. This can be considered a satisfactory result for analytical purposes whenever this behaviour does not deteriorate when practical rather than synthetic curves are considered. As for the first order

[1]Note: In Eqs. (1)–(3) the symbols used by the authors were maintained for all the parameters involved.

moment, the authors concluded that although the position of the mean is incorrectly predicted by the bi-G approximation, it might still qualify as a method for empirical prediction of retention time, better than $t_{R,p}$.

As far as the 2-G fitting function is concerned, the distorted experimental peak is considered as the convolution of two Gaussians in the whole range of z values so that the experimental peak is described by two sets of Gaussian moments:

$$h(V) = \frac{C_{inj}V_{loop}S}{v\sqrt{2\pi}}\left[\frac{\alpha_1}{\sigma_1}\exp\left(-\frac{1}{2}\left(\frac{t-(m_1)_1}{\sigma_1}\right)^2\right) + \frac{(1-\alpha_1)}{\sigma_2}\exp\left(-\frac{1}{2}\left(\frac{t-(m_1)_2}{\sigma_2}\right)^2\right)\right] \quad (4)$$

where:

- $C_{inj}V_{loop}$ is the injected mass of analyte;
- v is the eluent flow rate
- S is the sensitivity (peak area/mass injected);
- $(m_1)_1$ and $(m_1)_2$ are the first order moments of deconvolved Gaussian peaks 1 and 2;
- σ_1 and σ_2 are the square roots of peak variances;
- α_1 is the relative area of Gaussian peak 1

We selected this fitting function since we found that it satisfactorily fitted experimental chromatograms in some preliminary tests. In addition, the fact that the 2-G algorithm is available in some commercial curve-fitting programs makes it easy to use by unskilled operators.

2. Experimental

2.1. Equipment

The equipment used consisted of: a Dionex Series 4000i high-pressure pump for the eluents; a Dionex Series DX500 high-pressure pump for the post-column derivatization solution; a Dionex VDM-2 UV spectrophotometric detector coupled with a post-column derivatization module; a Dionex PED-2 conductivity detector coupled with a Dionex self-regenerating suppressor; a 250×4 mm and a 50×4 mm Dionex OmniPac PCX100, IC-cation analytical column, with sulphonic groups as cation-exchange sites (capacity 120 μeq/column); a 250×4 mm Dionex IonPac CS12, IC-cation analytical column, with carboxylic groups as cation-exchange sites (capacity 2.8 meq/column).

The eluents, the column and the post-column derivatization system were thermostated at 25±0.1°C. A flow-rate of 1 ml/min was used for all the eluents, and a flow-rate of 0.2 ml/min for the derivatization solution.

The following four configurations of the chromatographic system were adopted throughout our experiments:

1. pump/loop/column/detector;
2. pump/column/loop/detector;
3. pump/loop/column/chemical conditioning module/detector;
4. pump/column/loop/chemical conditioning module/detector.

2.2. Eluents

Working solutions were prepared at various concentrations in the range 0.1–0.5 *M*, by diluting a stock solution (0.5 *M* $HClO_4$). In the measurements performed at variable chloride concentrations, working solutions were obtained by mixing suitable volumes of $HClO_4$ and HCl ($[H^+]=0.22$ *M*). $MeSO_3H$ 8, 15, 30 and 45 m*M* was used for the elution of Li^+, Na^+, K^+, Cs^+ and Mg^{2+}. All the eluents contained 1% acetonitrile to ensure that the column packing was wetted properly.

2.3. Chemicals

Carlo Erba bidistilled water, Baker Instra-analyzed perchloric acid, Merck Suprapur hydrochloric acid, Fluka methanesulfonic acid and Baker analyzed acetonitrile were used in the eluent preparation. Aldrich 2-(5-bromo-2-pyridylazo)-5-diethylamino)-phenol, Baker analyzed Triton X-100, Baker analyzed boric acid and Baker analyzed sodium hydroxide were used for the derivatization solution.

2.4. Procedures

In the experiments concerning cadmium elution, 25 μl of a 5 ppm Cd^{2+} in 0.01 *M* HNO_3 solution were injected. Cd^{2+} detection was performed by means of the post-column derivatization system: a solution of 2-(5-bromo-2-pyridylazo)-5-diethyl-

amino)phenol (0.4 mmol at pH=10 by 0.5 *M* sodium borate–boric acid buffer) was mixed in a three-way tee at the column end, and the mixture was sent to the UV detector through a bead-packed reaction tube (the UV detector was set at 565 nm). The 25-cm PCX100 column was used for the elutions.

In the experiments concerning Li^+, Na^+, K^+, Cs^+ and Mg^{+2} the concentration of the injected solution was 8 ppm unless otherwise specified. The 5-cm PCX100 column coupled to the conductivity detector chain was used.

When NO_3^- was used as unretained solute, the UV detector was set at 210 nm, and water instead of a derivatization solution was injected into the chemical conditioning module according to configurations 2 or 3. The concentration of injected NO_3^- (as nitric acid) was 0.01 *M*.

2.5. Software

Galactic peak solve 1.02 (Galactic Industries) for Windows, and peak fitting module for MicroCal origin 4.1 (MicroCal) were used to perform peak fitting.

3. Results and discussion

3.1. The measurement of extra- and intra-column effects by using unretained solutes

Our methodological approach was firstly to check whether and to what degree of coverage the various fitting functions may represent the chromatographic peaks in the whole range of the experimental conditions used; then to test to what extent the relevant computed parameters followed a theoretical behaviour.

Fig. 1 shows how the shape of an IC peak (NO_3^- as unretained solute) varies according to the different configurations described in Section 2.1.

Table 1 shows the most significant findings concerning the elution of the unretained NO_3^- solute (cation exchange column) with the different chromatographic configurations, in order to estimate both intra and extra-column effects. V_0 and dead volumes along the eluent flow-line were: 0.201 and 1.05 ml for the 5- and 25-cm length chromatographic column respectively; 3 μl for both conductivity and spectrophotometric detector cells, 168 μl and 470 μl for their chemical conditioning module (CM), respectively. In computing *N*, the well-known equation: $N=(V_R/\sigma)^2=(V_R/0.425W_{1/2})^2$ where V_R is the retention volume and $W_{1/2}$ is the peak width at half-height, was used for both experimental and deconvolved peaks. This is certainly correct when dealing with non-skewed Gaussian peaks; it can however lead to an incorrect estimate of N_p, related to an experimental asymmetric peak.

With an unretained solute, σ_i as well as N_i refer to the extra-column effects (connecting tubes, loop, CM and detector cell dead volumes) when configuration 2 or 4 are used. When configurations 1 or 3 are used the effects of the pathways inside the chromatographic column (in the absence of exchange events) are also included. The extra-column effects depend both on the length of tubing regions where turbulent or laminar flows occur [5] and on the sequence of the components of the eluent flow-line. For instance inserting the column, before, instead of after the loop, causes (compare configurations 2 to 1, and 4 to 3 respectively in Table 1): (i) a decrease of 15–20% in asymmetry (a/b) and an ~80% decrease in σ_i in the absence of CM; (ii) a 15–20% decrease both in a/b and σ_i in the presence of CM.

A comparison between the features of configurations 1 and 3 (configuration 3 is the usual operating configuration) shows that the beneficial effect of the CM on the decrease of N_i (2.5 fold) and of a/b (2.2 fold) was counteracted by a 1.4–2 fold increase in σ_i. Since CM is inserted between the column and the detector, the above results show that: a/b is mostly generated before the column, that is in the loop and its connecting tubes, and is reduced by the CM; σ_i is mostly generated inside the column (compare configurations 1 and 2) and in the CM (compare configurations 1 and 3, and 2 to 4); N_i is mostly generated inside the column (due to its particular elution pathways) and is reduced by the CM (compare configuration 3 and 4).

As will be shown later, the injection of a retained solute will affect in an opposite way the σ_i and a/b values of the chromatographic set-up in the absence of exchange events in the column.

The contribution of the response time of the

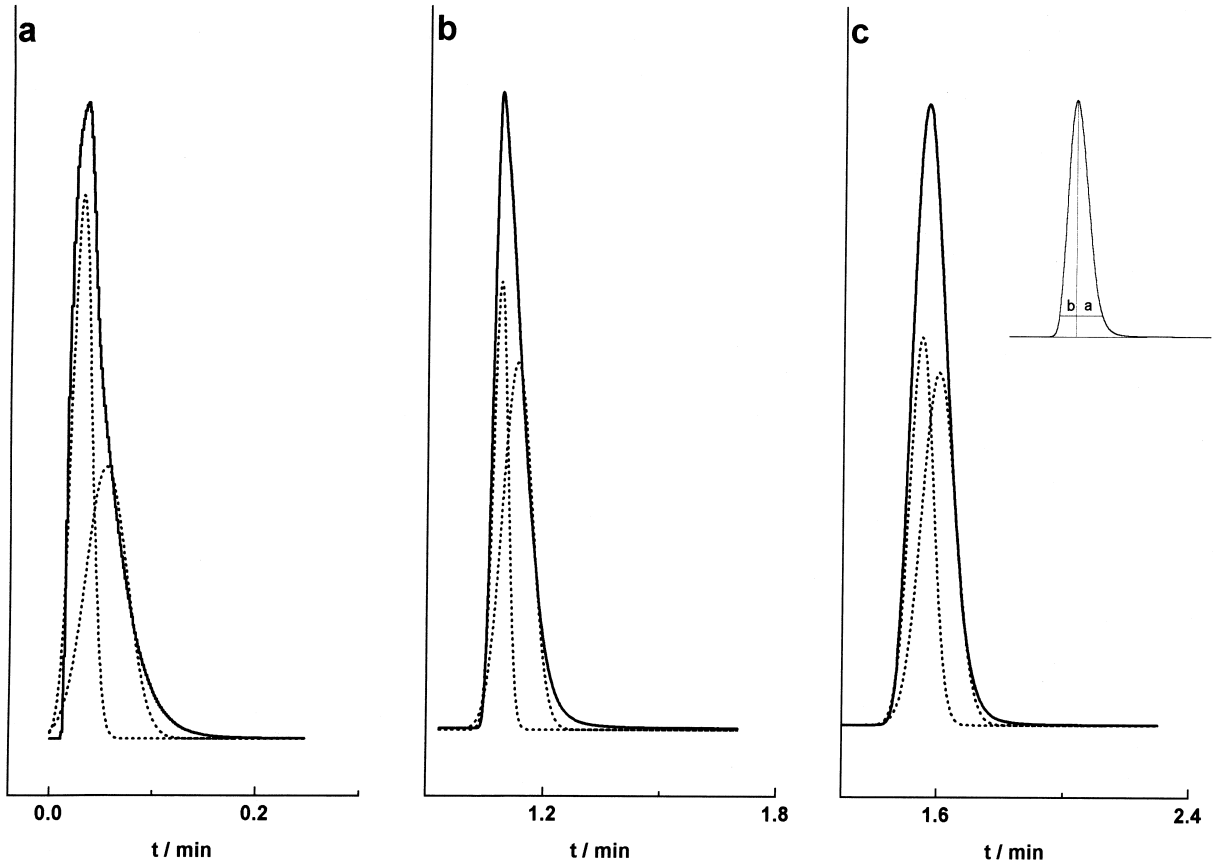

Fig. 1. Effect of various different chromatographic configurations on the shape of NO_3^- elution peak ($k'=0$). Curves a, b and c refer to configuration 2, 4 and 3 respectively (for the description of the configurations and of the chromatographic system used see Section 2). The two Gaussians curves computed according to the 2-G fitting function are also shown as a dotted line for each peak. The upper curve in (c) shows how asymmetry (a/b) was graphically computed at 0.1 h_{max}.

Table 1
Dependence on chromatographic configuration of: the asymmetry (a/b), the standard deviation (σ_i) and the theoretical plate number (N_i) of the original and deconvolved peaks according to the 2-G model (subscripts p, 1, 2 respectively) for unretained solutes in IC

Solute	Configuration[a]	σ_p	σ_1	σ_2	N_p	N_1	N_2	a/b
NO_3^-	1	0.034	0.018	0.036	998	3603	927	3.6
NO_3^-	2	0.016	0.010	0.020	3	8	6	3
NO_3^-	3	0.053	0.037	0.052	409	823	443	1.66
NO_3^-	4	0.044	0.031	0.043	129	244	149	1.44

[a] For the description of the various configurations see Section 2.1.
The values of σ_i, N_i, a/b refer to: (i) the solute dispersion generated inside the connection tube after the column (configurations 2 and 4); (ii) the solute dispersion in the flow line including the chromatographic column (configurations 1 and 3). The 250×4 mm PCX100 column coupled to a UV detector system and its CM was used.
N_i (i=1, 2 and p) values were computed according to the familiar equation: $N_i=((t_{R,i})/\sigma_i)^2$.

detector chain to the peak shape distortion, considered in [4], was assumed not to be significant in the present case. As can be seen from the curves in Fig. 1, the fronting edge is always steeper than the tailing edge. In curve (a) f.i., it takes 0.3 s to reach the 63.2% of the distance between zero and the maximum and 1.7 s to reach 63.2% of the same distance from the maximum to zero. In addition, normalised curves ($s(t)/s_{max}$ vs. t, where s is the actual signal) were found to be independent of concentration for both the solutes considered, Li^+ and Na^+, showing that the rise time of the signal was always lower than the detector chain rise time.

In spite of their formal diversity, all the experimental curves shown in Fig. 1 can be satisfactorily fitted by each of the three functions considered. Fig. 2 shows the computed and experimental curves relevant to the peak in Fig. 1a which was selected for its strong departure from a Gaussian. The first qualitative information that can be drawn comparing these curves is that the residuals appear to have the same distribution along the time axis, regardless of the type of the fitting function used. For a quantitative comparison the ability of the three functions to reproduce peak contour was tested by using the MicroCal Origin Peak Fitting Module. In this module, the same algorithm is used for error minimization so that any difference in the results, whenever significant, can be related to the diverse ability of the selected function in reproducing the shape of the peak considered. The values of χ^2 for the experimental conditions of Fig. 1a and c which represent very different peak shapes were in an increasing order: $1.01\cdot10^{-3}$ (EMG), $2.17\cdot10^{-3}$ (2-G), $6.61\cdot10^{-3}$ (bi-G) (Fig. 1a); $2.2\cdot10^{-5}$ (2-G), $4.6\cdot10^{-5}$ (EMG), $5.9\cdot10^{-5}$ (bi-G) (Fig. 1c). Assuming that such small differences in χ^2 are significant, the conclusion can be drawn that EMG fits Fig. 1a better than 2-G, namely a very distorted curve; 2G is better than EMG in the more frequent case of a not large peak asymmetry (Fig. 1c).

In terms of peak area, the values computed by using the three functions for each curve of Fig. 1 were referred to the numerically integrated experimental plot from the baseline of zero, using the trapezoidal rule. The following relative values were found (for EMG, 2-G and bi-G in the order): Fig. 1a: 1.028, 0.984, 0.981; Fig. 1b: 1.031, 0.961, 1.025; Fig. 1c: 1.023, 0.992, 0.991. That is when the same set of data is used every time for comparison, the 2-G leads to an estimate of the experimental area better than 99% in the case of moderately skewed peaks (Fig. 1c), as bi-G does, and it is better than EMG and bi-G for strongly asymmetric peaks.

Once the three fitting functions for the same set of data had been compared, measurements were performed to estimate the reproducibility of the parameters of the functions among replicates. Table 2 shows the most significant findings obtained from four replicate measurements of the Na^+ peak in IC. For τ, m_0, m_1 and σ ($m_2^{1/2}$), the C.V. was in the range 0.05–0.8%, with the highest value (2.5%) for $(m_0)_2$

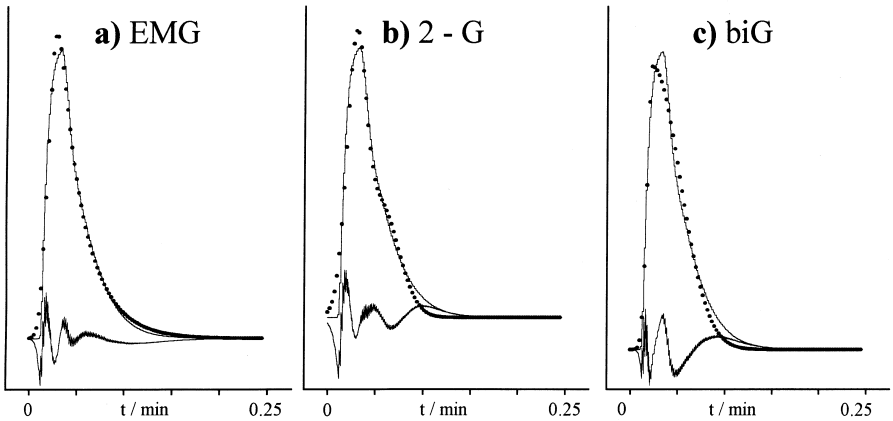

Fig. 2. Comparison between experimental and fitted contours for the peak of Fig. 1a. The fitted contours were computed according to: EMG (curve a), 2-G (curve b) and bi-G (curve c) functions. The residuals are also shown for each computed curve.

Table 2
Reproducibility of the estimated fitting parameters for EMG, 2-G and bi-G functions

		Replicates				Mean	C.V. (%)	I.C. ($\alpha=0.05$)
		1	2	3	4			
EMG	m_1	3.176	3.174	3.173	3.173	3.174	0.1	0.0017
	m_0	1.061	1.062	1.062	1.057	1.061	0.2	0.0022
	σ	0.058	0.057	0.058	0.057	0.058	0.4	0.0003
	τ	0.067	0.068	0.067	0.068	0.067	0.4	0.0003
	χ^2	$4.3\cdot10^{-4}$	$6.2\cdot10^{-4}$	$6.3\cdot10^{-4}$	$3.0\cdot10^{-4}$	$5.0\cdot10^{-4}$		
2-G	$(m_1)_1$	3.21698	3.21502	3.21369	3.21316	3.215	0.05	0.0017
	$(m_0)_1$	0.80092	0.8082	0.79221	0.79991	0.800	0.8	0.0064
	σ_1	0.06592	0.06568	0.06562	0.0656	0.066	0.2	0.0001
	$(m_1)_2$	3.31696	3.31866	3.31177	3.31489	3.316	0.1	0.0029
	$(m_0)_2$	0.26155	0.2552	0.2708	0.2588	0.262	2.5	0.0065
	σ_2	0.09835	0.09694	0.09826	0.09765	0.098	0.7	0.0006
	$(m_0)_t$	1.062	1.063	1.063	1.059	1.062	0.2	0.0021
	χ^2	$8.36\cdot10^{-4}$	0.00135	0.00122	$6.28\cdot10^{-4}$	$1.0\cdot10^{-3}$		
Bi-G	m_1	3.213	3.210	3.210	3.208	3.210	0.1	0.0017
	h_{max}	5.366	5.382	5.368	5.361	5.369	0.2	0.0089
	m_0	1.034	1.035	1.035	1.030	1.033	0.2	0.0021
	σ_1	0.062	0.061	0.062	0.061	0.061	0.6	0.0004
	σ_2	0.092	0.092	0.092	0.092	0.092	0.1	0.0001
	χ^2	$4.4\cdot10^{-3}$	$7.8\cdot10^{-3}$	$7.2\cdot10^{-3}$	$3.8\cdot10^{-3}$	$5.8\cdot10^{-3}$		

Number of replicates = 4. Solute considered: Na^+. Experimental conditions: configuration 4 (see Section 2.1), conductivity detector.

relevant to the second Gaussian of the 2-G model. The relatively higher C.V. of $(m_0)_1$ and $(m_0)_2$ computed according to 2-G rather than EMG, are related to the fact that there are eight parameters to optimize in the first case (four for each of the two Gaussians) rather than four as in the case of EMG. This small drawback is counteracted by the fact that the first order statistical moments $(m_1)_1$ and $(m_1)_2$ which are involved in thermodynamic studies are very reproducible (0.05–0.1%) for the 2-G, as well as the total peak area $(m_0)_t$. For instance from a comparison of peak areas, a perfect coincidence was found between EMG and 2-G total areas which were 3% higher than the bi-G total area. In addition, the 2-G algorithm is currently on the market in the form of various peak fitting programs which are easy to use for unskilled operators.

3.2. Dependence of σ_i, N_i and α_i on the capacity factor k_i'

In accordance with the aim of this research accurate correlations between $V_{R,i}$, $V_{0,i}$ and σ_i vs. k_i' need to be checked. This implies that V_R and V_0 have to be corrected for dead-volumes contribution, and σ_i for extra-column effects. In the following, corrected values will be identified by the subscript c. Eq. (5) highlights the dependence of $(\sigma_i)_c$ on k_i':

$$(\sigma_i)_c = V_{0,i}N_i^{-1/2} + V_{0,i}N_i^{-1/2}k_i' \quad (5)$$

where the subscript *i* refers to the experimental (p) or to the computed Gaussian curves.

In the above equation a linear relationship between $(\sigma_i)_c$ and k_i', regardless of the solute concentration, is expected whenever the same elution mechanism is involved. In this case the intercept and slope values will coincide. If $N_i^{-1/2}$ is left explicit in the second term only of the right-hand side of Eq. (5), the intercept can be expressed as $\sigma_{0,i}$ which is the S.D. of the solute peak when a volume $V_R = V_0$ has flowed through the chromatographic column. In fact, as will be shown below, $\sigma_{o,i}$ is a characteristic of a given chromatographic column only, regardless of the

solute and the salt composition of the eluent. $(\sigma_i)_c$ values can be obtained by subtracting $(\sigma_i)_b$ from any σ_i value, where $(\sigma_i)_b$ is the S.D. of the elution peak obtained according to configuration 4 using an unretained solute. Since the $(\sigma_i)_b$ value affects the intercept but not the slope in Eq. (5), the degree of coincidence between slope and intercept values will be a good test of the validity of the correction of extra-column effects. The additivity of both $\sigma_{o,i}$ and $(\sigma_i)_b$ to the S.D. due to the exchange mechanism inside the column, is related to the fact that these two terms are independent of k_i' and constant, as long as the chromatographic system does not change. Accurate values of N are then more correctly obtained from the slope, once the effective mobile phase volume of the column $V_{0,i}$ has been evaluated. In the case of non-linear isotherms or when the extracolumn effects hide (in the EMG model) the Gaussian component of the peak, N_i may appear to depend on k_i' so that the extrapolation to $k_i' = 0$ will be both uncertain and devoid of meaning.

Depending on whether ligands are present or not in the eluent, one of the following well-known equations was used [17] to estimate the shift of capacity factor of solute m_z with the change of eluent composition:

$$k_z' = {}^0k_z'([E])^{-m/n}\prod_j \gamma_j \quad (6)$$

$$(k_z')_{I,[E],[L]} = (k_z')_{I,[E]}\frac{[M_z]}{C_{M_z}} = \frac{(k_z')_{I,[E]}}{1 + \beta_1[L] + \beta_2[L]^2 + \cdots} \quad (7)$$

where m and n are the charges of the M_z solute and of the E competing ion, $[M_z]/C_{M_z}$ is the molar fraction of the free M_z ion in the eluent, ${}^0k_z'$ is the capacity factor of the z solute in the given chromatographic system at [E]=1, and $\prod_j \gamma_j$ is the activity coefficient product of the species undergoing equilibrium at the stationary–mobile interface. $\prod_j \gamma_j$ was found to be practically constant within a large ionic strength range [3]. For the sake of clarity, the charge of ligand L was omitted.

Two solute systems will be considered here in detail in order to find correlations between deconvolved peak parameters and the nature and concentration of both the solute and the eluent: the Cd^{+2}/Cl^- and the alkaline–alkaline earth systems.

3.2.1. Cd^{2+}/Cl^- system

In the case of Cd^{2+}, the shift of k_i' toward zero was obtained by increasing the Cl^- concentration, at a constant ionic strength and a constant concentration of competing ion ($H^+ = 0.22$ *M*) [3]: in the following the results obtained by the peak deconvolution into two Gaussians will be discussed every time before than those obtained by EMG or bi-G deconvolution.

3.2.1.1. The standard deviation of the Cd^{2+} peak

Fig. 3 shows that all σ_i vs. k_i' plots were linear over the whole range of Cl^- concentration ($r^2 \geq$

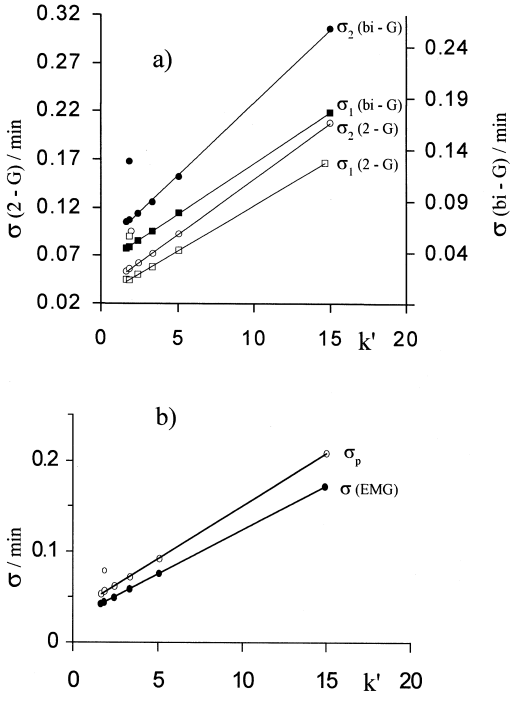

Fig. 3. σ_i vs. k_i' plots for the system Cd^{2+}/Cl^- at constant concentration of competing ion ($[H^+] = 0.22$ *M*) and variable Cl^- concentration. The regression equations were: (a): σ_2(bi-G)= 0.0142 k_2'+0.0433 (r^2=0.9991) (●); σ_1(bi-G)=0.0099 k_1'+ 0.0267 (r^2=0.9999) (■); σ_2 (2-G)=0.0122 k_2'+0.0360 (r^2= 0.9998) (○); σ_1 (2-G)=0.0095 k_1'+0.0269 (r^2=0.9997) (□); (b): σ_p=0.0116 k_p'+0.0339 (r^2=0.9999) (○); σ (EMG)=0.0098 k_{EMG}'+0.0262 (r^2=1) (●). The outlier values relevant to [Cl^-]= 0.22 *M* are also shown.

0.999) with the exception of the highest Cl^- concentration value for which both the experimental k'_p and σ_p as well as k'_i, σ_1 and σ_2 of the 2-G model in addition to σ_2 of the bi-G model are higher than expected. The k'_i values were computed using the $t_{R,p}$ for the experimental curve (relevant to the maximum of the peak) and the first moment of the deconvolved peaks for EMG, 2-G and bi-G. The fact that for the highest chloride concentration both k'_i and most of the σ_i values in σ_i vs. k'_i plots show outlier values, is not related to the Cd^{2+}/Cl^- system itself. It was actually shown that at a constant ionic strength ($I=0.22$) and when the ClO_4^- molar fraction is lower than 0.09, the characteristics of the column–eluent system change regardless of the solute, as observed by a sharp change in V_0, the mobile phase volume inside the chromatographic column [3]. The linearity of each σ_i vs. k'_i plot shown in Fig. 3 implies that according to Eq. (5), N_i does not depend on k'_i. Note that the slope of σ_i vs. k'_i plots is practically the same for σ_1 (2-G), σ_1 (bi-G) and σ (EMG): $(97\pm1)\cdot10^{-4}$; a mean slope of 0.0119 ± 0.0002 is obtained in σ_p and σ_2 (2-G) vs. k' plots. Besides, the constant slope in σ_i vs. k'_i plots implies that the relevant N_i values are practically coincident assuming $V_{0,1}$ be the same. It must be emphasized that N values computed from $t_{R,p}$ and σ_p values give a rough information on the efficiency of the column.

3.2.1.2. Peak asymmetry a/b, relative area α_1 and time constant τ

Both a/b and the relative area values $\alpha_1=A_1/A$ (A=total area; A_1=area of Gaussian peak 1) were found to be independent of k'_i and specifically $a/b=1.4$ (R.S.D.=2.5%) and $\alpha_1=0.55$ (R.S.D.=4%), with the exception of the i values relevant to the highest Cl^- concentration, where a/b, as well as σ_i, presents a sharp variation ($a/b=2.5$). In the EMG deconvolution, τ shows a nearly linear trend vs. k' (see Fig. 5a) and a distinct variation at the highest Cl^- concentration. In agreement with the expectations [11] the ratio τ/σ for the EMG function was found to be constant as well (mean value 1.042, R.S.D. 7.5%). Thus, in addition to the other findings [3] τ vs. k' plots provide a further objective indication of when the elution process is no longer controlled by the same exchange equilibrium.

3.2.1.3. k'_i shift and stability constant (β_j) determination

If k'_1 and k'_2 both follow the theoretical shift with Cl^- concentration, Eq. (7) can be written in the form [3,17]:

$$(k'_{I,[Cl^-],[H^+]})_i=(k'_{I,[H^+]})_i\left(\sum_{j=0}^{n}\beta_j[Cl^-]^j\right)^{-1} \quad (8)$$

As for the deconvolution into Gaussian peaks 1 and 2 (2–9), from Eq. (8), one has:

$$\frac{(k'_{I,[Cl^-],[H^+]})_1}{(k'_{I,[Cl^-],[H^+]})_2}=\frac{(k'_{I,[H^+]})_1}{(k'_{I,[H^+]})_2}=\text{const.}=R \quad (9)$$

Actually, R values were found to be constant in the whole range of Cl^- concentrations (at constant C_{H^+}), in agreement with Eq. (9): $R=1.02$, R.S.D.=1.2%. Table 3 shows β_1 and β_2 values for the system Cd^{2+}/Cl^-, separately estimated from k'_i sets of data. A comparison of the various sets of data highlights that β_i values computed by using the different fitting models do not differ significantly. As for bi-G in particular, β_1 values practically coincide with those computed by other fitting models, whereas β_2 values (which are more prone to be affected by small errors occurring in the computation of m_1) significantly differ from them. We assume therefore that the convergence between β_i values computed by the EMG and 2-G models (which have a completely different approach) is a test of their individual ability to provide an accurate estimate of stability constants. β_i values computed by the experimental retention time are not too far from the EMG and 2-G values: this may be related to the fact that in the experimental conditions used, the peak asymmetry remains

Table 3
Estimate of β_1 and β_2 stability constants for the system Cd^{2+}/Cl^- ($I=0.22$) according to the m_1 values derived from the experimental or deconvolved peaks

	β_1	β_2	r^2
Experimental peak	27.89	64.95	0.99990
2-G deconvolution (peak 1)	28.53	59.01	0.99998
2-G deconvolution (peak 2)	28.59	58.98	0.99998
EMG deconvolution	28.86	57.96	0.99998
Bi-G deconvolution	28.99	53.92	0.99999

constant in the whole range of retention times tested. The rather scarce ability of bi-G to give correct first-order moment values was foreseen by Buys and de Clerk [16], as previously mentioned. The occurrence of erratic values in the experimental asymmetry a/b values, k_p and σ_p (in addition to σ_2 (bi-G) and τ as well as σ_1 (2-G) and σ_2 (2-G)) as a function of chloride concentration highlights that intra-column effects (other elution mechanisms in addition to ion exchange) are significant [3]. It would be interesting to test other complexing agent–cation systems or other columns to establish whether accurate β_i constants are obtained at a higher peak distortion than that observed.

These kinds of tests, in addition to the others discussed in [3] and the control that the free uncomplexed cation only is involved in the exchanges between phases [18], makes for the first time, the IC method highly competitive with other instrumental methodologies, in obtaining accurate β values. In the absence of these tests, the results may be either accurate or completely wrong without the possibility of checking the size of the error (see Table 1 in ref. [2]). The superior feature of IC is that—under well defined conditions, for which different objective tests are allowable—the variable m_1 only depends on the α free cation fraction of the solute considered. In potentiometry f.i. the measured variable ΔE includes the junction potential which can vary with ligand concentration, while the need to convert ionic activity into concentration for the free cation species which is in reversible electrochemical equilibrium at the electrode interphase is a drawback; the same happens in calorimetry when mixing enthalpies and heat exchange with the surroundings are additive to complex formation enthalpy.

In terms of a comparison between the three deconvolution approaches in the evaluation of β values, it can be concluded that EMG and 2-G lead to convergent results. The 2-G approach has, however, the distinct advantage that the central moments of both the relevant deconvolved peaks can be easily estimated and concur in improving the quality of information. In the EMG approach, only the first moment of the Gaussian component of the peak, and not the τ constant, are suitable for β evaluation. In addition, as for the EMG and bi-G fitting, data processing must be matched by general mathematical programmes. Finally in the bi-G, both the first and second order moments of the peak are not directly related to the peak shape which is described (according to Eq. (2)) by $t_{R,p}$, (z_m in Eq. (2)) σ_1 and σ_2 of the first and second half-Gaussian curves.

3.2.2. The alkaline and alkaline-earth element series

In the experiments described above, the shift of k_i' for Cd^{2+} was obtained by suitably changing the eluent composition. Additional experiments were then performed by using Li^+, Na^+, K^+, Cs^+ and Mg^{2+} as solutes and at four different concentrations of hydrogen ion as the competing ion.

From the whole set of experiments concerning the alkaline series it was found that:

3.2.2.1. σ_i

σ_i linearly increases with k_i' regardless of the type of solute and the competing ion concentration C_{H^+}, starting from $\sigma_b + \sigma_o$. Fig. 4a and b show as an example σ_p, σ_2 (2-G) and σ (EMG) vs. k_i' plots, for k_i' ranging from 2 to 30. A σ_p value for Mg^{2+} equal to 0.89 (not shown in Fig. 4a), estimated from the regression equation, is comparable with the experimental value which was equal to 1.01: the small discrepancy, which includes the possible effects of a doubly charged solute and a very long retention time ($k_p' = 200$; $t_R = 40.34$ min at $[H^+] = 45$ mM), can be considered acceptable f.i. when predicting peak contour as a function of the eluent composition.

The regression equations for σ_i vs. k_i' plots were respectively: $\sigma_p = 0.0042\ k_p' + 0.0151$ ($r^2 = 0.998$); σ_1 (2-G) $= 0.0029 \cdot k_1' + 0.0166$ ($r^2 = 0.959$); σ_2 (2-G) $= 0.0042\ k_2' + 0.0304$ ($r^2 = 0.971$) for the 2-G model; σ_1 (bi-G) $= 0.0029\ k_{bi\text{-}G}' + 0.0134$ ($r^2 = 0.944$) and σ_2 (bi-G) $= 0.0058 \cdot k_{bi\text{-}G}' + 0.0222$ ($r^2 = 0.984$) for the bi-G model; σ (EMG) $= 0.0028\ k_{EMG}' + 0.0109$ ($r^2 = 0.969$) for the EMG model. Note that σ_1 (2-G), σ_1 (bi-G) and $\sigma_{(EMG)}$ have practically the same slope vs. k' (0.00287 ± 0.0003), as occurred for Cd^{2+}/Cl^- system. The slope of both σ_p and σ_2 (2-G) vs. k' plot for the alkaline series is 0.0042. The linear dependence of σ_i on k_i' implies that N_i is independent of k_i' and of the type of solute and only related to the peculiar features of the chromatographic column. These results showing that N (and consequently the plate height H) is independent of k_i', are in contrast

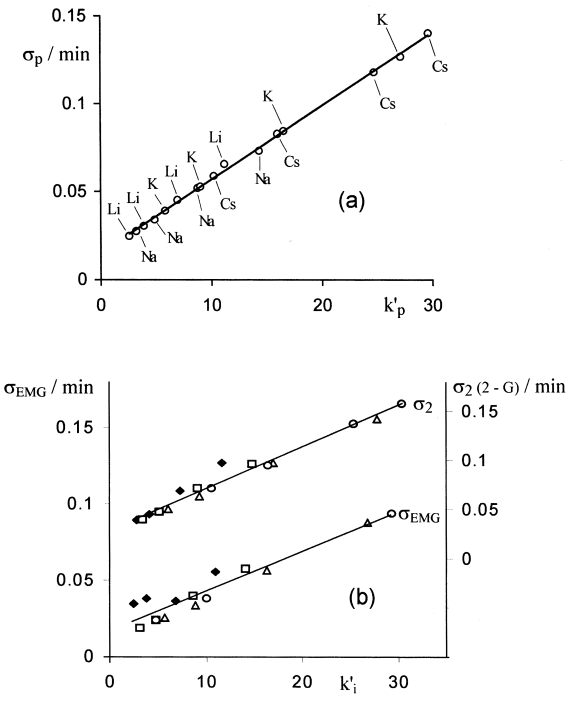

Fig. 4. Some examples of linear relationships in the σ_i vs. k_i' plots for the alkaline series at four different concentrations of the competing ion ([H^+]=8, 15, 30 and 45 m*M*): (a) σ_p vs. k_p' plot; (b) σ_2 (2-G) vs. k' and σ (EMG) vs. k' plots for Li^+ (♦), Na^+ (□), K^+ (△) and Cs^+ (○) solutes. The regression equations were: $\sigma_p = 0.0042\ k_p' + 0.0151$ ($r^2 = 0.998$). σ_2 (2-G) $= 0.0042\ k_2' + 0.0304$ ($r^2 = 0.970$); σ (EMG) $= 0.0028\ k_{EMG}' + 0.0109$, ($r^2 = 0.969$).

with other authors' findings [6] relevant to gas-chromatographic measurements. According to these authors, the effect of dead volumes at the injector end on *H* (and consequently σ^2) was lower when a heavily retained solute (heptane) was used instead of a lightly retained one (methane): it is however unclear whether the t_R and $W_{1/2}$ values used to compute *N* (and *H*) were corrected respectively for dead volume retention time and extra-column effects or not. Besides the statement of these authors that post-column dead volumes do not affect the shape of the chromatographic peak as much as pre-column dead volumes, is in agreement with the results previously discussed about the effect of the different configurations of the chromatographic line.

3.2.2.2. a/b

Fig. 5(b) shows that *a*/*b* linearly decreases in the lower k_p' range and apparently reaches a limiting value depending on the nature of the solute. The couples of solute Li^+ and Na^+, K^+ and Cs^+,

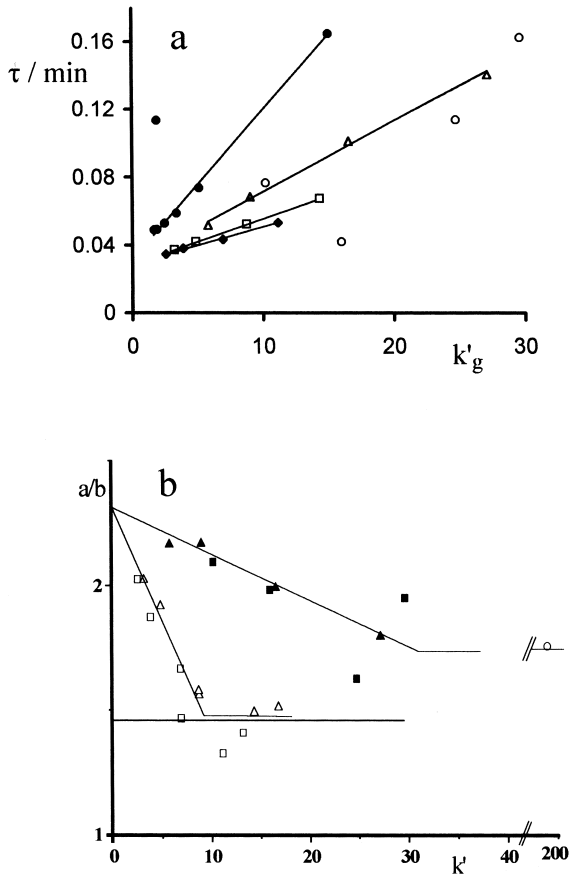

Fig. 5. (a) τ vs. k_{EMG}' plots for Cd^{2+} (●), Li^+ (♦), Na^+ (□), K^+ (△) and Cs^+ (○). k_{EMG}' values for each solute refer to the different concentrations of the competing ion ([H^+]=7, 8, 15, 30 and 45 m*M*). Regression parameters: $\tau = 0.0088\ k_{EMG}' + 0.0313$ ($r^2 = 0.9976$) for Cd^{2+}; $\tau = 0.0021\ k_{EMG}' + 0.0294$ ($r^2 = 0.997$) for Li^+; $\tau = 0.0027\ k_{EMG}' + 0.0287$ ($r^2 = 0.999$) for Na^+; $\tau = 0.0041\ k_{EMG}' + 0.0301$ ($r^2 = 0.998$) for K^+. (b): *a*/*b* vs. k_p' plots for Li^+ (□), Na^+ (△), K^+ (▲) and Cs^+ (■). The *a*/*b* value for Mg^{2+} (○) is also shown (*a*/*b* = 1.8). *a*/*b* and k_p' values for most of the solutes were measured at five different concentrations of the competing ion ([H^+]=7, 8, 15, 30 and 45 m*M*). The continuous line parallel to the k' axis refers to *a*/*b* values obtained for the system Cd^{2+}/Cl^- at [H^+]=0.22 *M* and variable Cl^- concentration using a different chromatographic system.

respectively present similar behaviour. In particular, the a/b limiting value for K^+ and Cs^+ coincides with that measured for Mg^{2+} ($k'=200$): this supports the hypothesis that a/b really tends to a limit.

It is likely that a/b is a constant for Mg^{+2} in the whole range of k'_p values considered (2–200) as found for Cd^{+2} (continuous line in Fig. 5b). Unfortunately higher concentrations of competing ion (and consequently lower k'_p values) could not be tested for Mg^{+2} since they were not compatible with the background conductivity suppressor. Yet in all cases, the original asymmetry of the chromatographic configuration, which can be obtained by using an unretained solute, tends to be cancelled out both by the increase in k' of the solute and by some peculiar characteristics of the solute itself involved in the exchange processes, perhaps its hydrophilicity or charge density. It is these peculiarities that affect the rate of change of a/b with k'_p. The intercept, which gives the asymmetry of the chromatographic system for $k'_p=0$ was 2.3 ± 0.05, for all the solutes.

3.2.2.3. τ

When τ is plotted vs. k' (see Fig. 5(a)), it linearly increases (while a/b decreases) with a slope which depends on the nature of the solute (similarly to a/b). Fig. 5(a) also shows τ vs. k' curve of Cd^{2+} for comparison.

3.2.2.4. α_i

The relative areas of the deconvolved peaks α_i according to the 2-G model appear to be similarly dependent on the nature of the solute as a/b, when the concentration of the competing ion is changed. As far as Li^+ and Na^+ are concerned, two distinct curves are obtained by plotting α_1 vs. k'_1 values: in both cases α_1 linearly increases with k'_1 ($0.028\ k'_1+0.572$ for Li^+ and $0.0139\ k'_1+0.598$ for Na^+) in the range of k'_1 values considered. The curves for K^+ and Cs^+ are statistically indistinguishable and show a negative slope near to zero (-0.003). In spite of such different behaviours the extrapolated α_1 values (to $k'_1=0$) were practically coincident for all the solutes considered ($\alpha_1=0.58$; R.S.D.$=2\%$). The extrapolated value corresponds to the relative area value that would be obtained at $k'_1=0$, using the same chromatographic configuration.

Should the above results be supported by further IC experiments performed with other types of columns, the following findings would hold as far as the 2-G fitting model, which was never tested before in IC, is concerned:

–any chromatographic peak can be satisfactorily deconvolved into two Gaussians;

–in spite of the empirical approach used in peak deconvolution, $(m_1)_i$, σ_i and α_1 are related to k'_i through simple relationships;

–for a given chromatographic column in a given instrumental configuration, standard reference plots can be built up for a selected number of solutes of interest, by using a few different concentrations of competing ions in the eluent. The intercepts and the slopes of these m_i vs. k'_i reference plots can thus be obtained;

–by using the well-known Eq. (6) or Eq. (7), new values of k'_z are computed for the different z solutes at any selected composition of the eluent, whether ligands are present or not;

–for each set of new k'_z data, $(m_1)_i$, σ_i and α_1 are computed from the reference plots so that the individual shape of the z peak can be predicted according to Eq. (10):

$$h(V)=\sum_{j=a}^{z}\left\{\frac{C_{inj}V_{loop}S}{v\sqrt{2\pi}}\left[\frac{\alpha_1}{\sigma_1}\times\exp\left(-\frac{1}{2}\left(\frac{t-(m_1)_1}{\sigma_1}\right)^2\right)+\frac{(1-\alpha_1)}{\sigma_2}\times\exp\left(-\frac{1}{2}\left(\frac{t-(m_1)_2}{\sigma_2}\right)^2\right)\right]\right\}_j \quad (10)$$

α_1, $(m_1)_1$, $(m_1)_2$, σ_1 and σ_2 can be computed by the reference plots once the actual k' value has been estimated.

In the case of EMG a similar equation derived from Eq. (1) can be easily obtained.

4. Conclusions

Several experiments were performed in IC by changing (i) the sequence of the components in the

chromatographic eluent flow-line; (ii) the concentration of the competing ion and the type of retained solutes with the aim of checking when and to what extent, the deconvolution of the experimental peak could be successfully performed according to different functions.

By using an unretained solute ($k'=0$), it was possible to reach a better understanding of the influence that each component the chromatographic set-up, including the column with its particular pathways, has on the peak shape in the absence of ion exchange events. We found that (a) asymmetry and N_i are mainly generated in the precolumn dead volumes and sharply decrease, by about 50%, when the chemical conditioning module (CM) is inserted before the detector chain; (b) the insertion of the chromatographic column gives rise to a ~20% increase in a/b; and (c) σ_i is mainly generated in the column and post-column dead volumes, though it increases owing to the insertion of the CM (see Table 1).

Three fitting functions (EMG, 2-G and bi-G) were used and their ability was tested to (i) accurately and reproducibly fit the area and the contour of peaks with different asymmetry; (ii) give sound information on the degree of agreement between the shift of the experimental retention time $t_{R,p}$ and the thermodynamic expectations.

It was found that:

(i) as far as Cd^{2+}/Cl^- system is concerned, EMG and 2-G lead to practically coincident values of β_1 and β_2. This perfect agreement among the results, if confirmed by further experiments, can be explained by assuming that both these fitting functions, in spite of the different approaches used, are able to overcome the drawbacks of the effects that the distortion of the experimental peak has on $t_{R,p}$. Consequently while the use of one of them will suffice in giving correct thermodynamic information, using both will help in validating the results.

(ii) The use of the bi-G function, as already observed by [16] is less efficient when the first order statistical moment is the variable of interest.

(iii) The fact that β_i values computed by the experimental retention time are not far from the ones computed by EMG or 2-G can be explained by the fact that the asymmetry a/b (graphically measured), as well as τ/σ (computed according to the EMG model) were found constant over the whole range of $t_{R,p}$ variation. In terms of reproducibility among replicates of the computed parameter m_1 involved in β_i determination, the C.V. was always lower than 0.2% for all the fitting functions.

All these findings show that, as far as peak distortion effects are concerned, the accurate determination of stability constants by IC can be performed by using EMG or 2-G fitting functions. The additional possibility to test whether the elution mechanisms is changed owing to too large variations in the eluent composition [3] or to parallel exchange equilibria [18], makes IC very competitive with other instrumental techniques in the determination of stability constants.

The correct prediction of the dependence of $(m_1)_i$ on some thermodynamic properties of the eluent composition and the observed linear dependence of σ_i on $(m_1)_i$ through k_i', allows one to correctly compute the contour of the peak of a given solute for any composition of the eluent. This is important when stability constants are known for each of the metal ions which are to be separated by IC in a mixture. In this case it is sufficient to measure the values of $(m_1)_i$ and σ_i for some solutes at a few eluent compositions however selected. With a suitable computer programme, such as the one built up in our laboratory, an optimized mixture of ligands, each at a suitable concentration, is found for which the separation of the experimental solute peaks is obtained at the desired resolution.

Acknowledgements

The financial support of MURST and CNR is gratefully acknowledged.

References

[1] J.C. Giddings, Dynamics of Chromatography Part I: Principles and Theory, Marcel Dekker, New York, 1965.
[2] P. Janoš, J. Chromatogr. 641 (1993) 229.
[3] P. Papoff, A. Ceccarini, P. Carnevali, J. Chromatogr. A 706 (1995) 43.
[4] L.J. Schmauch, Anal. Chem. 31 (1959) 225.
[5] V. Maynard, E. Grushka, Anal. Chem. 44 (1972) 1427.
[6] H.W. Johnson Jr., F.H. Stross, Anal. Chem. 31 (1959) 357.

[7] K.I. Sakodynsky, L.V. Streltzov, V.Yu. Zelvensky, S.A. Volkov, I.N. Rozhenko, Anal. Chem. 45 (1973) 1557.
[8] E.V. Dose, S. Jacobson, G. Guiochon, Anal. Chem. 63 (1991) 833.
[9] R.E. Pauls, L.B. Rogers, Anal. Chem. 49 (1977) 625.
[10] W.W. Yau, Anal. Chem. 49 (1977) 395.
[11] E. Grushka, Anal. Chem. 44 (1972) 1733.
[12] W.E. Barber, P.W. Carr, Anal. Chem. 53 (1981) 1939.
[13] I.G. McWilliam, H.C. Bolton, Anal. Chem. 41 (1969) 1755.
[14] E. Grushka, G.C. Monacelli, Anal. Chem. 44 (1972) 484.
[15] H.M. Gladney, B.F. Dowden, J.D. Swalen, Anal Chem. 41 (1969) 883.
[16] T.S. Buys, K. de Clerk, Anal. Chem. 44 (1972) 1273.
[17] P.R. Haddad, P.E. Jackson, Ion Chromatography, Principles and Applications (Journal of Chromatography Library, Vol. 46), Elsevier, Amsterdam, 1990, p. 133.
[18] P. Hajos, G. Revesz, C. Sarzanini, G. Sacchero, E. Mentasti, J. Chromatogr. A 640 (1993) 15.